JBC RESEARCH ARTICLE

Cellular retinoid-binding proteins transfer retinoids to human cytochrome P450 27C1 for desaturation

Received for publication, July 22, 2021, and in revised form, August 25, 2021 Published, Papers in Press, September 1, 2021,
https://doi.org/10.1016/j.jbc.2021.101142

Sarah M. Glass and F. Peter Guengerich*

From the Department of Biochemistry, Vanderbilt University School of Medicine, Nashville, Tennessee, USA

Edited by Ruma Banerjee

Cytochrome P450 27C1 (P450 27C1) is a retinoid desaturase expressed in the skin that catalyzes the formation of 3,4-dehydroretinoids from all-*trans* retinoids. Within the skin, retinoids are important regulators of proliferation and differentiation. *In vivo*, retinoids are bound to cellular retinol-binding proteins (CRBPs) and cellular retinoic acid–binding proteins (CRABPs). Interaction with these binding proteins is a defining characteristic of physiologically relevant enzymes in retinoid metabolism. Previous studies that characterized the catalytic activity of human P450 27C1 utilized a reconstituted *in vitro* system with free retinoids. However, it was unknown whether P450 27C1 could directly interact with holo-retinoid-binding proteins to receive all-*trans* retinoid substrates. To assess this, steady-state kinetic assays were conducted with free all-*trans* retinoids and holo-CRBP-1, holo-CRABP-1, and holo-CRABP-2. For holo-CRBP-1 and holo-CRABP-2, the k_{cat}/K_m values either decreased 5-fold or were equal to the respective free retinoid values. The k_{cat}/K_m value for holo-CRABP-1, however, decreased ∼65-fold in comparison with reactions with free all-*trans* retinoic acid. These results suggest that P450 27C1 directly accepts all-*trans* retinol and retinaldehyde from CRBP-1 and all-*trans* retinoic acid from CRABP-2, but not from CRABP-1. A difference in substrate channeling between CRABP-1 and CRABP-2 was also supported by isotope dilution experiments. Analysis of retinoid transfer from holo-CRABPs to P450 27C1 suggests that the decrease in k_{cat} observed in steady-state kinetic assays is due to retinoid transfer becoming rate-limiting in the P450 27C1 catalytic cycle. Overall, these results illustrate that, like the CYP26 enzymes involved in retinoic acid metabolism, P450 27C1 interacts with cellular retinoid-binding proteins.

Vitamin A, also called all-*trans* retinol (atROL), and other natural and synthetic derivatives of vitamin A are collectively referred to as retinoids. *In vivo*, atROL can be sequentially metabolized by dehydrogenases to form all-*trans* retinaldehyde (vitamin A aldehyde, atRAL) and all-*trans* retinoic acid (vitamin A acid, atRA), the biologically active form of retinoids in the cell (retinoid metabolism is summarized in Fig. 1). In cells, there exist two types of retinoid-binding proteins, cellular retinol-binding proteins (CRBPs) and cellular retinoic acid–binding proteins (CRABPs). These small proteins are members of the intracellular lipid-binding protein superfamily, which bind hydrophobic ligands within an internal β-barrel cavity (1). In humans, there are four isoforms of CRBPs that bind atROL and atRAL and two isoforms of CRABPs that bind atRA (2). Because retinoids bind to these proteins tightly, and retinoid-binding proteins are generally expressed in concentrations that exceed their ligands, it is expected that little to no free all-*trans* retinoids exist within the cell (2). Cellular retinoid-binding proteins mediate retinoid function and metabolism within the cell by delivering retinoids specifically to receptors and metabolic enzymes. In addition, the ratio of apo-CRBP (without retinoid bound) to holo-CRBP (with retinoid bound) has been shown to regulate retinoid metabolism within the cell. The most well-studied example of this is in the formation and breakdown of retinyl esters, the storage form of retinoids. Lecithin retinol acyltransferase (LRAT) catalyzes the esterification of fatty acyl groups to the terminal hydroxyl group of atROL. atROL can be released from retinyl esters through hydrolysis by retinyl ester hydrolase. The activity of LRAT is inhibited by excess apo-CRBP-1 (3), and the activity of retinyl ester hydrolase is stimulated (4), leading to increased amounts of available atROL. This activity of apo-CRBPs is not thought to be due to retinoid-binding capabilities, given that chemically modified CRBP-1 that can no longer bind atROL still inhibits LRAT (3). This apo:holo-CRBP regulation is thought to provide a mechanism to control retinoid availability within the cell (2).

The ability of P450s to interact with retinoid-binding proteins has previously been illustrated with P450 26B1 and 26C1, which can utilize atRA bound to CRABP-1 or CRABP-2 (holo-CRABPs) as substrates (5, 6). Cytochrome P450 (P450 or CYP) enzymes are members of a superfamily of heme-containing monooxygenases responsible for approximately 95% of all reported oxidation reactions (7). Humans have 57 P450 genes with varying functions and substrate specificities. P450s are involved in the metabolism of steroids, fatty acids, xenobiotics (pharmaceutical drugs and carcinogens), eicosanoids, and also have important roles in the metabolism of all fat-soluble vitamins, that is, vitamins A, D, E, and K (8). Direct channeling of atRA from holo-CRABPs to CYP26s has been proposed. Excess apo-CRABPs were also shown to inhibit P450 26B1 and 26C1 metabolism, and it was proposed that this was through allosteric modulation or inhibition, not through retinoid

* For correspondence: F. Peter Guengerich, f.guengerich@vanderbilt.edu.

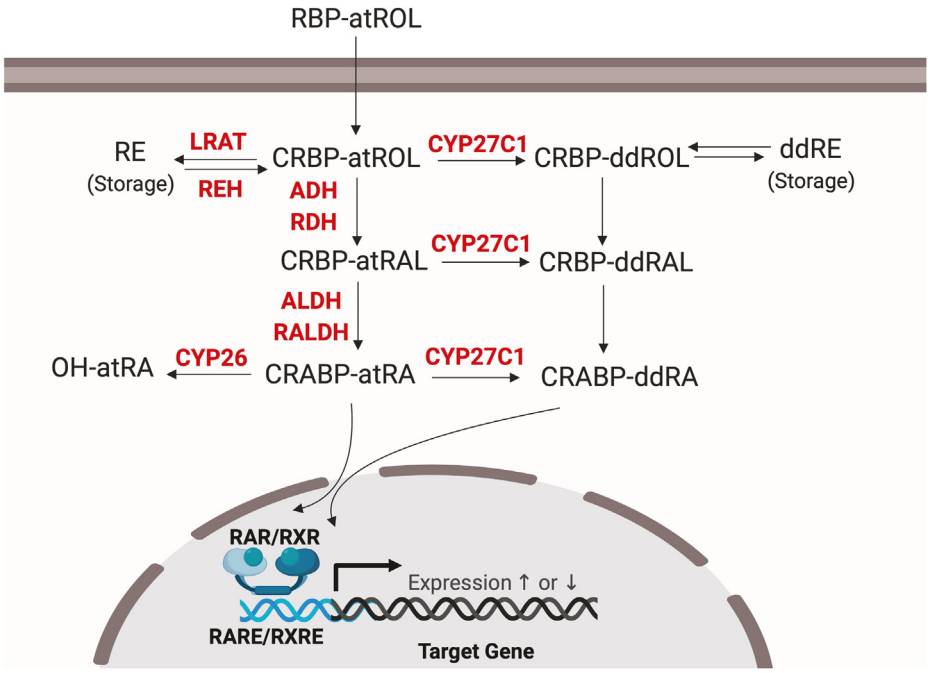

Figure 1. Retinoid metabolism within the cell. The all-*trans* retinoid metabolic pathways are adapted from Roos *et al.* (69). The proposed role of P450 27C1 in the desaturation of all-*trans* retinoids is shown. Figure created in BioRender.com. ADH, alcohol dehydrogenase; ALDH, aldehyde dehydrogenase; atRA, all-*trans* retinoic acid; atRAL, all-*trans* retinaldehyde; atROL, all-*trans* retinol; CRABPs, cellular retinoic acid–binding proteins; CRBPs, cellular retinol-binding proteins; ddRA, 3,4-dehydroretinoic acid; ddRAL, 3,4-dehydroretinaldehyde; ddROL, 3,4-dehydroretinol; LRAT, lecithin retinol acyltransferase; RALDH, retinaldehyde dehydrogenase; RAR/RXR, retinoic acid/retinoid X receptor; RARE/RXRE, retinoic acid/retinoid X responsive element; RBP, retinol-binding protein; RDH, retinol dehydrogenase; RE, retinyl ester; REH, retinyl ester hydrolase; CYP, cytochrome P450.

sequestration or competition for binding to the P450. Notably, P450s 3A4 and 2C8, P450s that had been shown to metabolize free atRA *in vitro*, do not utilize holo-CRABPs as substrates (5), suggesting that this interaction is P450 specific and that not all P450s identified as *in vitro* retinoid metabolizers may be as relevant for retinoid metabolism *in vivo*.

P450 27C1 was recently characterized as an all-*trans* retinoid desaturase (Fig. 2) expressed in the skin (9, 10). Previous studies that identified and characterized the ability of P450 27C1 to convert all-*trans* retinoids to 3,4-dehydroretinoids utilized a reconstituted *in vitro* system with free retinoids. Whether or not P450 27C1 is able to accept retinoid substrates from cellular retinoid-binding proteins is currently unknown. 3,4-Dehydroretinoid levels have been correlated with levels of cellular retinoid-binding proteins, but the role of these proteins in 3,4-dehydroretinoid formation is unknown (11, 12). Potential regulation of 3,4-dehydroretinoid formation by excess apo-CRBPs has also not been assessed.

In this work, we addressed the hypothesis that human P450 27C1 interacts with three cellular retinoid-binding proteins expressed in the skin (13, 14)—CRBP-1, CRABP-1, and CRABP-2—to directly receive retinoid substrates (channeling) or if ligand dissociation from the retinoid-binding protein is required as would be predicted by the free ligand model (Fig. 3). Channeling in this case refers to the direct transfer of retinoid from the holo-cellular retinoid-binding protein to the P450 without free diffusion into the bulk solution. *In vitro* steady-state kinetic experiments and isotope dilution channeling assays were performed with purified recombinant P450 27C1 and cellular retinoid-binding proteins to distinguish between these two models. These interactions are further characterized through substrate-binding assays and mutagenesis.

Results

Assessing holo-CRBPs as substrates for P450 27C1 retinoid desaturation

To determine if P450 27C1 can directly accept retinoid substrates from cellular retinoid-binding proteins, P450 27C1 steady-state kinetics assays were performed with holo-CRBPs (atROL–CRBP-1, atRAL–CRBP-1, atRA–CRABP-1, and atRA–

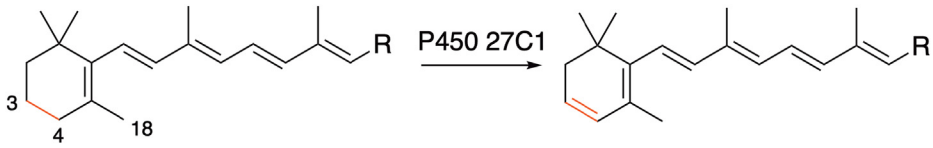

Figure 2. 3,4-Desaturation of all-*trans* retinoids by P450 27C1. Relevant carbon atoms to this work are numbered (70). Minor 3- and 4-hydroxylation products are also formed (9). Substrates are as follows: R = CH_2OH, all-*trans* retinol (vitamin A); R=CHO, all-*trans* retinaldehyde (vitamin A aldehyde); R = COOH, all-*trans* retinoic acid (vitamin A acid). P450, cytochrome P450.

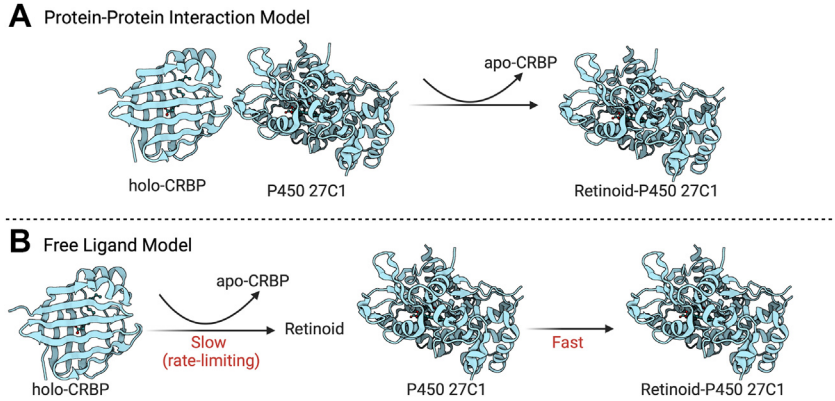

Figure 3. Potential mechanisms of retinoid transfer from holo-CRBPs to P450 27C1. *A*, protein–protein interaction model: holo-CRBP interacts directly with P450 27C1 and transfers retinoid substrate. *B*, free ligand hypothesis model (indirect transfer): retinoid dissociates from holo-CRBP, and free retinoid can then bind to P450 27C1. Figure created in BioRender.com. CRBP, cellular retinoid-binding protein; P450, cytochrome P450.

CRABP-2) prepared with a retinoid:CRBP ratio of 1:1. Reactions were run with the free substrates in parallel. Values for the k_{cat} and k_{cat}/K_m for the reactions were calculated from hyperbolic fits to the data for the rate of dehydroretinoid formation against substrate concentration (free retinoid, or holo-CRBP) (Fig. 4 and Table 1). For atROL–CRBP-1 and atRAL–CRBP-1, the specificity constant (k_{cat}/K_m) was similar to the respective free retinoids, while the k_{cat} was slightly lower (68% and 74% of the free retinoid for atROL–CRBP-1 and atRAL–CRBP-1, respectively), and the K_m values were not different. For atRA–CRABP-2, the k_{cat}/K_m was 5-fold lower because of a 36% decrease in k_{cat} and a 3-fold increase in K_m. For atRA-CRABP-1, these changes were even more substantial: the k_{cat}/K_m was decreased 65-fold, k_{cat} was decreased 10-fold, and K_m was increased 7.5-fold. To determine whether the amount of desaturation that occurred in the reactions with the holo-CRBPs as substrates was due to channeling or only metabolism of the free retinoid available in solution, kinetic values were calculated based on the amount of free substrate that would be present, given the reported binding affinity of the CRBPs for retinoids (Fig. S4). For atROL–CRBP-1, atRAL–CRBP-1, and atRA–CRABP-2, the amount of product formed was higher than what would be expected if P450 27C1 was only able to oxidize the free retinoid in reaction. For atRA–CRABP-1, the amount of 3,4-dehydroretinoic acid (ddRA) formed does not exceed the free ligand prediction. These steady-state kinetic results suggest that atROL–CRBP-1, atRAL–CRBP-1, and atRA–CRABP-2 channel retinoids to P450 27C1, but atRA–CRABP-1 does not.

Direct channeling of retinoids from holo-CRBPs to P450 27C1

Isotope dilution experiments were performed to examine the differences in atRA delivery to P450 27C1 by CRABP-1 and CRABP-2. In these assays, free d_5-all-*trans* retinoic acid was added along with an equal concentration of a holo-CRABP with d_0-all-trans retinoic acid bound. If no channeling of retinoid to the P450 occurs, dissociation from the CRABP is required and the product formed from the free retinoid (added to the reaction) should be much higher than the amount of product formed from the retinoid bound to the CRABP. Conversely, if channeling occurs, the amount of product formed from each retinoid should be similar.

With CRABP-1 (Fig. 5*A*), the amount of product formed from the free atRA was much higher than that from the holo-CRABP. Notably, the ratio of free:bound product formation also decreased over time, which would be expected as the retinoid originally bound to the CRABP dissociated and

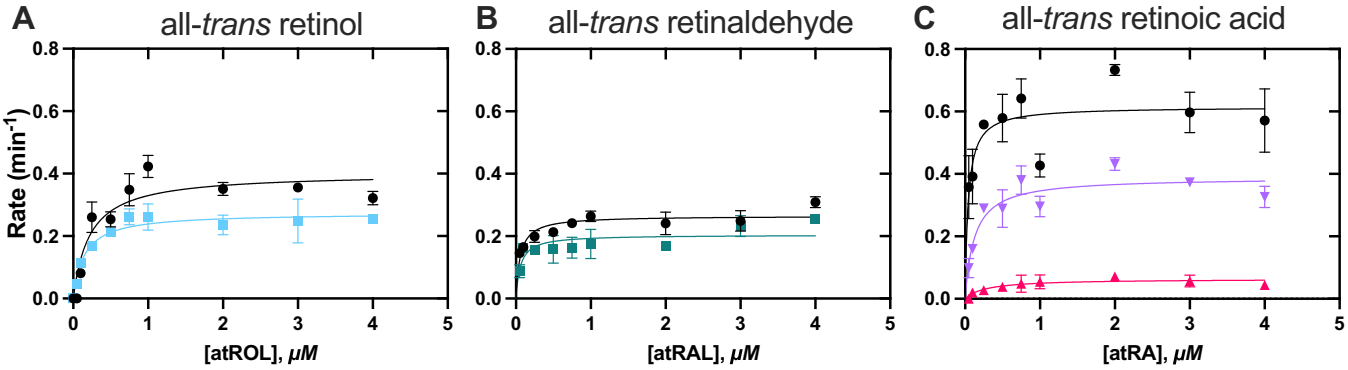

Figure 4. Effects of CRBPs on P450 27C1 retinoid desaturation. Steady-state kinetics of 3,4-dehydroretinoid formation from (*A*) all-*trans* retinol bound to CRBP-1 (□); (*B*) all-*trans* retinaldehyde bound to CRBP-1 (■); (*C*) all-*trans* retinoic acid bound to CRABP-1 (▲) or CRABP-2 (▼) or as a free substrate (●). Reactions were done in duplicate, and points are shown as the means ± SD (range). Samples were analyzed by UPLC-UV. CRBP, cellular retinol-binding protein; CRABP, cellular retinoic acid-binding protein; P450, cytochrome P450; UPLC-UV, ultraperformance liquid chromatography-ultraviolet detection.

Table 1
Kinetic parameters of retinoid desaturation with holo-CRBP or free retinoid by P450 27C1

Substrate	K_m (μM)	k_{cat} (min^{-1})	k_{cat}/K_m (μM^{-1} min^{-1})
atROL	0.22 ± 0.06	0.40 ± 0.03	1.8 ± 0.5
atROL–CRBP-1	0.15 ± 0.03	0.27 ± 0.01	1.9 ± 0.4
atRAL	0.06 ± 0.01	0.27 ± 0.01	5 ± 1
atRAL–CRBP-1	0.06 ± 0.02	0.20 ± 0.01	4 ± 1
atRA	0.04 ± 0.02	0.61 ± 0.03	15 ± 5
atRA–CRABP-1	0.3 ± 0.1	0.064 ± 0.008	0.23 ± 0.09
atRA–CRABP-2	0.12 ± 0.03	0.39 ± 0.02	3.1 ± 0.7

Results are from experiments done in duplicate. Parameters were estimated using a hyperbolic fit in GraphPad Prism that solved for k_{cat} and k_{cat}/K_m directly.

exchanged with the retinoid in solution (Fig. 5*C*). With CRABP-2, the amount of product formed from both the free and bound retinoid was more similar, and the ratio of product formation remained largely the same over time (Fig. 5, *B* and *C*). This result is consistent with what would be expected for direct retinoid delivery between the CRABP and the P450. Overall, the results from these isotope dilution channeling experiments support the differences in channeling observed in steady-state kinetic analyses with holo-CRABP-1 and holo-CRABP-2.

Rate of retinoid transfer from holo-CRABPs to P450 27C1

Stopped-flow binding studies were performed to compare the rate of free retinoid binding to P450 27C1 to the rate of retinoid transfer from holo-CRABPs to P450 27C1 (Fig. 6). In preliminary experiments, adrenodoxin (Adx) was found to increase the rate of free retinoid binding to P450 27C1, and accordingly, Adx was included in the k_{on} rate determinations with free retinoid (Fig. S6). With free atRA, the k_{on} was 278 ± 5 μM^{-1} min^{-1} (*i.e.*, 4.6×10^6 M^{-1} s^{-1}). The transfer of retinoids from holo-CRABPs to P450 27C1 was much slower, as evidenced by the time scale required to saturate P450 27C1 binding (Fig. 6*B*).

The patterns with the CRABP-1 and CRABP-2 retinoic acid complexes were different. The CRABP-2 complex showed a distinctive multiphasic behavior (Fig. 7, *A* and *B*). The rates with the complexes were measured with varying concentrations of P450 27C1, and as expected, the amplitude of the final P450–retinoic acid complex increased with the P450 concentration in both cases. With the CRABP-1 complex, the plots could be fit with single exponentials of 0.0020 to 0.0034 s^{-1}, which are very close to the reported CRABP-1 k_{off} rate in the literature (Table S3, (15)). The plots of the CRABP-2 data were fit much better with biexponential fits (Fig. 7, *C* and *D*). The goodness of fit with the single exponential is illustrated by the residuals plot in Figure 6*D*. The fast phase, which accounted for 25 to 38% of the reaction, was much faster than the reported CRABP-2 k_{off} rate (Table S3, (15)) but much slower than the binding of free retinoic acid by P450 27C1 (Fig. 6*A*). We interpreted the equilibria in the context of the scheme in Figure 7*E*. The CRABP-1 system was dominated by the k_{off} rate (0.0020–0.0034 s^{-1}). For the CRABP-2 system, the equilibrium was more complex, as indicated by the biphasic behavior at all P450 concentrations. This was interpreted as a faster conversion to a P450–CRABP-2–retinoic acid ternary complex, which then undergoes a slower rearrangement to a complex in which the retinoic acid has been delivered to the P450 active site to produce the type I spectral change (observable by the ΔA_{390}-A_{420} difference). However, we did not have enough boundary conditions to further model the individual steps in this complex system.

Attempts to identify the P450 27C1–CRABP interaction interface

Cross-linking experiments were performed in attempt to characterize potential P450–CRABP complex formation. No cross-links were detected between P450 27C1 and apo-CRABPs or holo-CRABPs (data not shown). Because of this, no downstream applications (*i.e.*, in-gel digestion and LC-MS/MS analysis) could be used to identify potential residues that mediated the P450 27C1–CRABP interaction.

CRABP sequences and holo-CRABP structures were compared with one another to identify residues that may allow for differential interactions with P450 27C1 (Fig. S8). There was one predominant area, the residues surrounding the entrance to the ligand-binding site, where differences between

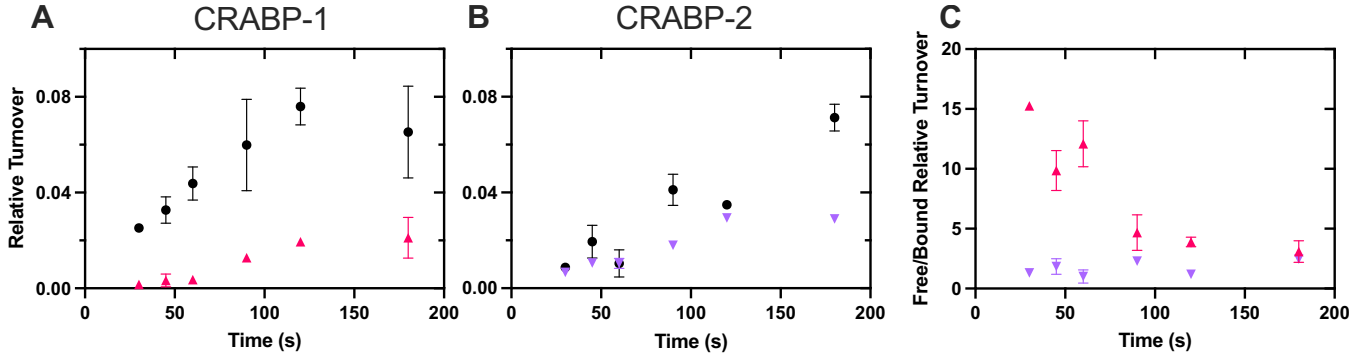

Figure 5. Differential channeling of all-*trans* retinoic acid from CRABPs to P450 27C1. Isotope dilution experiments with free d_5-all-*trans* retinoic acid and d_0-all-*trans* retinoic acid bound to (*A*) CRABP-1 and (*B*) CRABP-2. Relative product formation from the free retinoid (●) and the holo-CRABP (▲ CRABP-1 and ▼ CRABP-2) is shown in each panel. *C*, ratio of free:bound product formation as a function of time for CRABP-1 (▲) and CRABP-2 (▼). Reactions were done in duplicate, and points are shown as the means ± SD (range). Samples were analyzed by LC-MS/MS. P450, cytochrome P450; CRABPs, cellular retinoic acid–binding proteins.

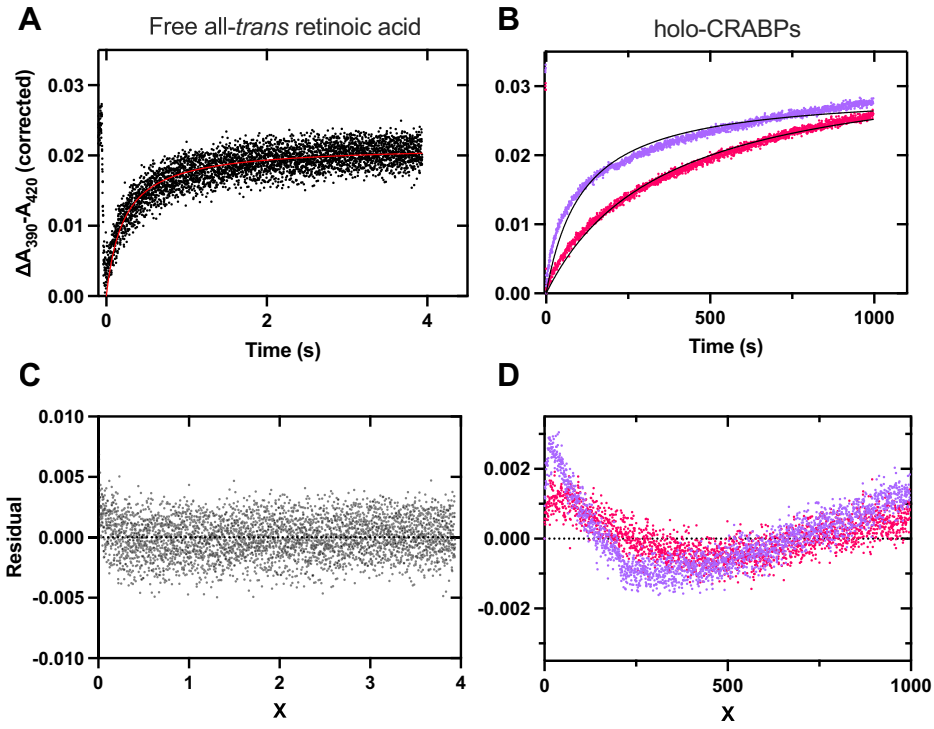

Figure 6. Stopped-flow mixing transients of all-*trans* retinoic acid substrate mixing with P450 27C1. P450 27C1 (1 μM, final) was mixed with (*A*) free (●) and (*B*) CRABP-1-bound (●) or CRABP-2-bound (●) all-*trans* retinoic acid (all 1 μM, final) in 200 mM potassium phosphate (pH 7.4). *C*, residuals plot for panel *A*. *D*, residuals plot for panel *B*. Free all-*trans* retinoic acid data are the average of six replicate shots, holo-CRABP data are from a single shot. The *line* in each panel is a single-exponential fit to the data (see Experimental procedures). Apparent k_{on} values: free all-*trans* retinoic acid, 278 ± 5 μM^{-1} min^{-1}; holo-CRABP-1, 0.169 ± 0.001 μM^{-1} min^{-1}; holo-CRABP-2, 0.539 ± 0.005 μM^{-1} min^{-1}. CRABPs, cellular retinoic acid–binding proteins; P450, cytochrome P450.

the two structures were noted. To determine if these residues were key in mediating the interaction with P450 27C1, two mutant CRABPs were made, where the residues of one protein were swapped with the residues from the other. Steady-state kinetics assays with these holo-CRABP mutants (CRABP-1 Q75E/P81K/K102E and CRABP-2 E75Q/K81P/E102K) were performed, but the results were similar to those observed for the WT proteins (Fig. S9).

Effects of apo-CRBPs on P450 27C1 activity

To examine the potential regulation of P450 27C1 activity by apo-CRBPs, reactions were performed with each retinoid and the respective retinoid-binding protein (Fig. 8). atROL desaturation was inhibited by excess apo-CRBP-1, but this inhibition plateaued (Fig. 8*A*). No inhibition was observed for atRAL desaturation (Fig. 8*B*), and atRA desaturation was inhibited by both apo-CRABP-1 and apo-CRABP-2 with no product formation at a >2-fold molar excess of apo-CRABP (Fig. 8*C*). K_i values calculated for inhibition of desaturation of atROL by apo-CRBP-1 or atRA by apo-CRABPs ranged from 0.025 to 0.21 μM (Table 2).

To determine if apo-CRBPs were general inhibitors of P450 27C1 desaturation or if apo-CRBPs could compete with holo-CRBPs for binding to P450 27C1, apo-CRPB inhibition assays were completed with CRBPs that did not bind the retinoid in the reaction (*i.e.*, CRABPs with atROL and atRAL, CRBP-1 with atRA) (Fig. 9). Reactions that were initiated with free substrates were designed to examine the general capacity for apo-CRBPs to inhibit desaturation (Fig. 9, *A*–*C*). Reactions initiated with holo-CRBPs were done to measure the potential for apo-CRBPs to compete for binding (Fig. 9, *D*–*F*). No inhibition was observed unless the apo-CRBP was able to bind the retinoid in the reaction.

Discussion

P450 27C1 has been identified as a retinoid desaturase (10, 16). In fish and amphibians, the retinoid desaturase activity of P450 27C1 has an important physiological role in red-shifting photoreceptor sensitivity and allowing these organisms being able to see longer wavelength light (16). Human P450 27C1 performs the same reactions *in vitro* (10), and its localization to the skin has been identified (9), but the contribution of human P450 27C1 to retinoid desaturation *in vivo* has not been determined. The function of dehydroretinoids within the skin, where they constitute approximately one-fourth of the retinoid pool (17), is also not well understood. In this work, we sought to assess the potential contribution of P450 27C1 to retinoid desaturation *in vivo* and provide additional insight into the regulation and formation of dehydroretinoids, in the context of individual retinoid-binding proteins.

P450 27C1 is able to interact with holo-CRBP-1 and holo-CRABP-2 to receive all-*trans* retinoid substrates for metabolism. Based on the steady-state kinetics of product formation (Fig. 4) and isotope dilution experiments (Fig. 5), the observed patterns of product formation can only be explained by direct channeling of the retinoid substrate from the

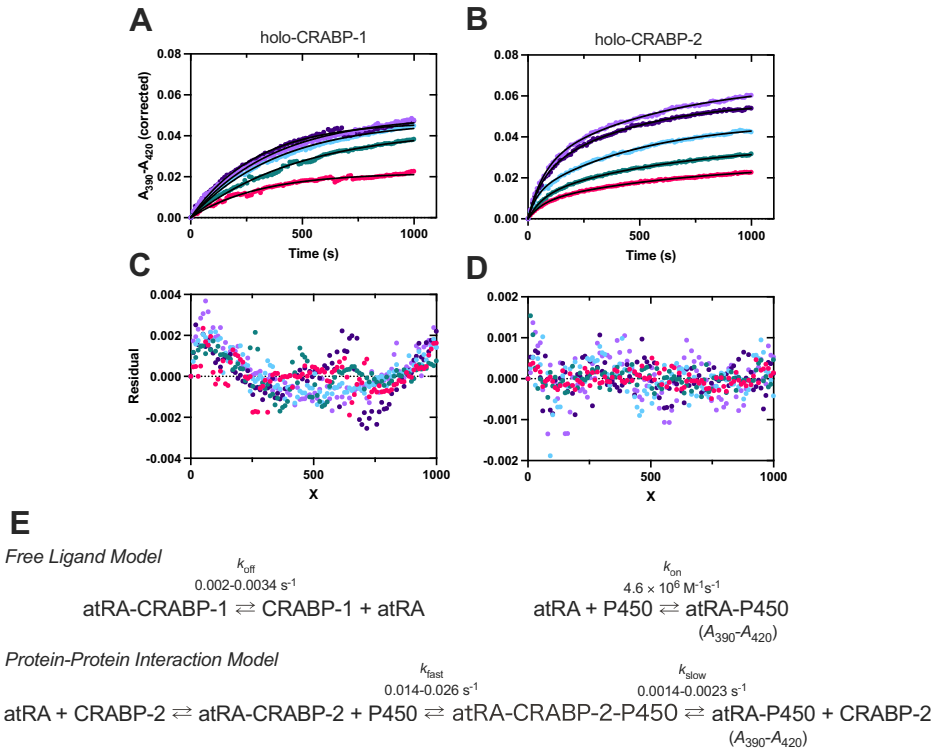

Figure 7. All-*trans* retinoic acid transfer rate dependence on P450 27C1 concentration. *A*, CRABP-1 fits. P450 27C1 concentration was varied (1–5 μM), and the data were fit to a single exponential, with rates varying from 0.0025 to 0.0034 s^{-1}. *B*, residual plot for panel *A*. *C*, CRABP-2 fits. The P450 27C1 concentration was varied (1–5 μM), and the data were fit to a biexponential equation, with rates of the fast phase (25–38% of the reaction) varying from 0.014 to 0.026 s^{-1}. *D*, residual plot for panel *C*. *E*, scheme of proposed equilibria involved in the reactions in Figures 6 and 7 (*A–D*). CRABP, cellular retinoic acid–binding protein; P450, cytochrome P450.

holo-binding protein to the P450 in that metabolism of only the free retinoid in the reaction would result in lower amounts of product formation (Fig. S4). Catalytic assay results suggest that holo-CRABP-1 does not channel atRA to P450 27C1 (Figs. 4 and 5). Rates of atRA transfer from the holo-CRABPs to P450 27C1 also support the conclusion about channeling with CRABP-2 but not CRABP-1 (Figs. 6 and 7). Within the context of retinoid metabolism in the skin, the lack of interaction between P450 27C1 and CRABP-1 likely does not negatively affect the potential contribution of P450 27C1 to retinoid desaturation. CRABP-2 is the predominant CRABP expressed in the skin, and some reports describe little to no expression of CRABP-1 (13, 18). P450 27C1 therefore could access most, if not all, of the all-*trans* retinoids present in the skin.

In all reactions with holo-CRBPs as the substrate, the catalytic rate (k_{cat}) was decreased in comparison with the respective free substrates (Table 1). Previous studies have proposed that the decrease in catalytic rate observed with holo-retinoid-binding proteins is due to the rate of retinoid transfer from the binding protein to metabolic enzyme

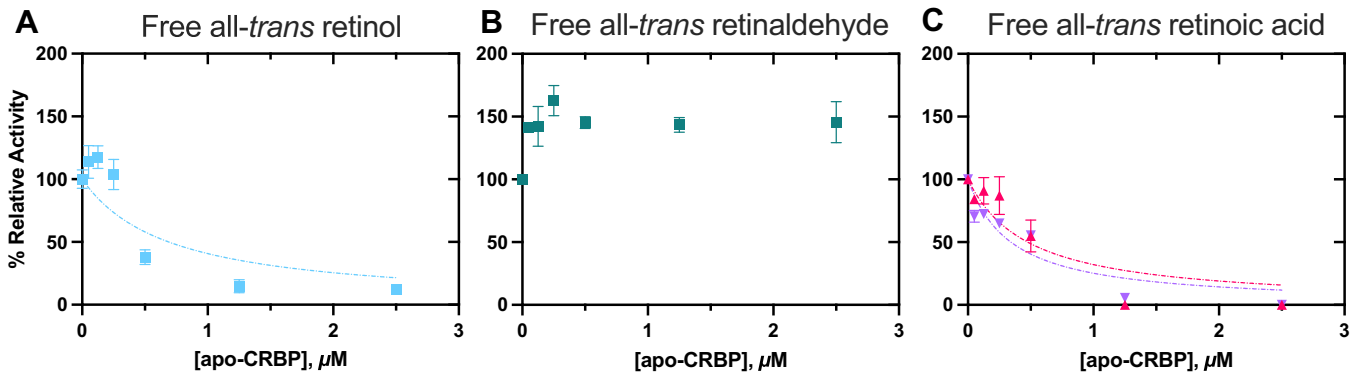

Figure 8. Effect of excess apo-CRBPs on 3,4-dehydroretinoid formation by P450 27C1. Incubations with excess apo-CRBPs were performed with (*A*) all-*trans* retinol; (*B*) all-*trans* retinaldehyde; and (*C*) all-*trans* retinoic acid (0.5 μM, added as free substrate). Reactions contained apo-CRBP-1 (▫, ■), apo-CRABP-1 (▲), or apo-CRABP-2 (▼) up to 5× the concentration of the retinoid in the reaction (0.05–2.5 μM, final). Reactions were done in duplicate, and points are shown as the means ± SD (range). Activity is relative to a point that did not contain apo-CRBP. Samples were analyzed by UPLC-UV. CRABPs, cellular retinoic acid–binding proteins; CRBPs, cellular retinol-binding proteins; P450, cytochrome P450.

Table 2
Inhibition of P450 27C1 retinoid desaturation by excess apo-CRBPs

Retinoid	Apo-CRBP	K_i (μM)
atROL	CRBP-1	0.21 ± 0.08
atRAL	CRBP-1	Not detected[a]
atRA	CRABP-1	0.03 ± 0.01
	CRABP-2	0.025 ± 0.005

Results are from experiments done in duplicate. Parameters were estimated using the Morrison K_i equation in GraphPad Prism with data from Figure 8.
[a] No inhibition was observed with excess apo-CRBP-1 with all-*trans* retinaldehyde.

becoming rate-limiting in the reaction (2). To our knowledge, this has been proposed, but rates of transfer have not been determined. Given that substrate binding to P450s is readily observable and that we have previously determined the rates of several steps of the P450 27C1 catalytic cycle (Fig. 10) (9), we addressed the question of whether retinoid transfer became rate limiting for P450 27C1 through UV-visible spectroscopy (Figs. 6 and 7). The apparent k_{on} values of retinoid transfer from holo-CRABPs to P450 27C1 are much slower than the rate of free retinoid binding (Fig. 6). In addition, these rates are on the same order of the observed k_{cat} for the reaction (Table 1), suggesting that retinoid transfer may be rate limiting. In addition, no kinetic burst with holo-CRBPs was observed (Fig. S7), as in the case with free all-*trans*-retinol as a substrate (9), indicating that a step after product formation did not become rate limiting (*i.e.*, step 9 in Fig. 10).

We observed specificity in the interaction of cellular retinoid-binding proteins with P450 27C1. P450 27C1 can accept retinoid substrates from holo-CRBP-1 and holo-CRABP-2 but not holo-CRABP-1. There are minor differences between the two CRABP proteins studied (77% identity, 93% similarity), and attempts were made to identify the potential P450–CRABP interaction interface. Interactions between holo-CRBPs and retinoid-receiving proteins are often transient and have been difficult to detect (19–21). Cross-linking was selected as a potential experimental method to trap the proteins together for structural characterization. The approach has previously been used to study interactions between P450s and their catalytic redox partners. 1-Ethyl-3-(3-dimethylaminopropyl)carbodiimide hydrochloride (EDC) is often used because of the presence of primary amines on the proximal P450 surface and abundance of carboxylic groups on the redox partner surface (22–25). CRABPs, like NADPH-P450 reductase, cytochrome b_5, and Adx also have many carboxylic acid groups on their surfaces, so a similar cross-linking approach was utilized. Although P450 27C1 was able to form cross-links with Adx, as expected, no cross-links were detected between P450 27C1 and CRABPs (data not shown). Lack of chemical cross-linking has also previously been reported with CRABP-2 and retinoic acid receptor (RAR) (15). This was attributed to the transient nature of the interaction between the two proteins. We believe that the interaction

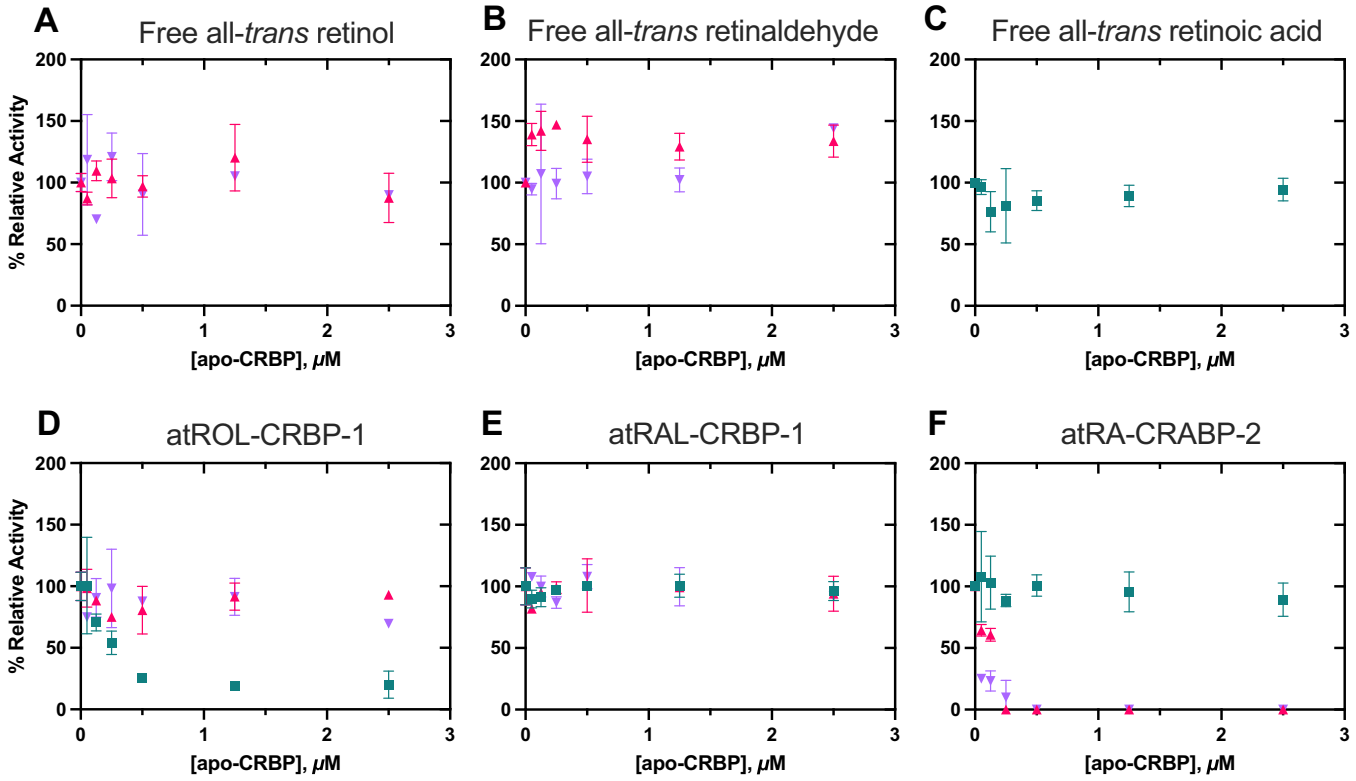

Figure 9. Apo-CRBP inhibition of P450 27C1 does not occur through general allosteric modulation or competition with holo-CRBPs. Incubations with excess apo-CRBPs were performed with free substrate (0.5 μM): (*A*) all-*trans* retinol; (*B*) all-*trans* retinaldehyde; and (*C*) all-*trans* retinoic acid or with holo-CRBP (0.5 μM) (*D*) atROL-CRBP-1; (*E*) atRAL-CRBP-1; (*F*) atRA-CRABP-2. Reactions contained apo-CRBP-1 (■), apo-CRABP-1 (▲), or apo-CRABP-2 (▼) up to 5× the concentration of the retinoid in the reaction (0.05–2.5 μM, final). Reactions were done in duplicate, and points are shown as the means ± SD (range). Activity is relative to a point that did not contain apo-CRBP. Samples were analyzed by UPLC-UV. atRA, all-*trans* retinoic acid; atRAL, all-*trans* retinaldehyde; atROL, all-*trans* retinol; CRABPs, cellular retinoic acid–binding proteins; CRBPs, cellular retinol-binding proteins; P450, cytochrome P450.

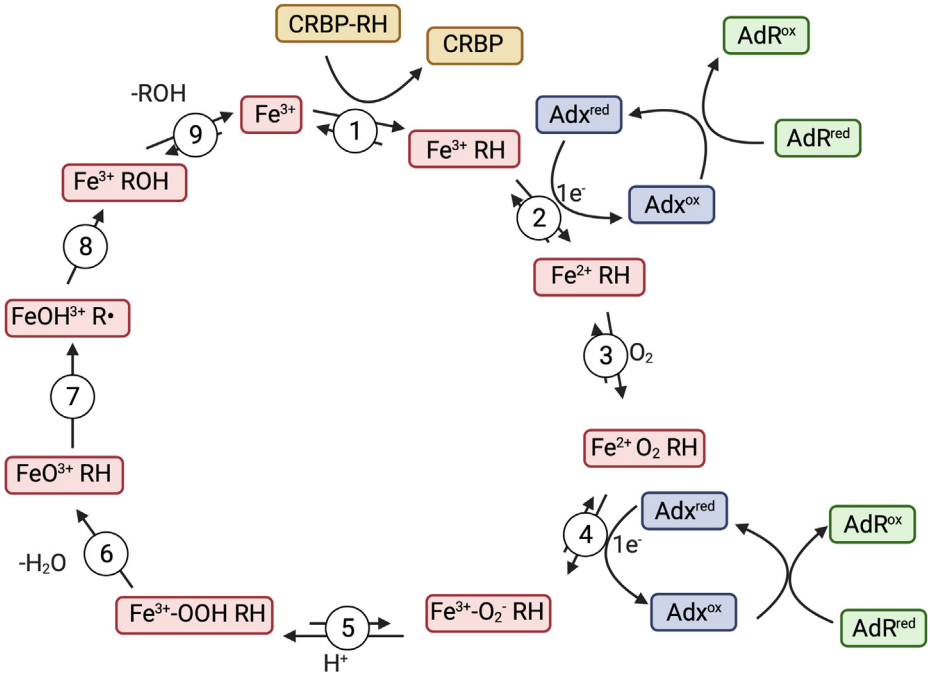

Figure 10. Proposed catalytic cycle for P450 27C1 with CRBPs. Steps are indicated with numbers. Rates for steps 1 (with free retinoid binding), 2, 7, and 9 were previously measured, and steps 2 (reduction by Adx) and 7 (hydrogen abstraction) were determined to be partially rate limiting (9). With holo-CRBPs, step 1 (retinoid transfer) becomes rate limiting, leading to the observed decreases in k_{cat}. Figure created in BioRender.com. AdR, NADPH–Adx reductase; Adx, adrenodoxin; CRBPs, cellular retinol-binding proteins; P450, cytochrome P450.

between P450 27C1 and the cellular retinoid-binding proteins may also be transient. Other efforts (gel filtration, UV-visible spectroscopy, zonal elution chromatography) were made to observe physical binding but were unsuccessful (data not shown).

Accordingly, mutagenesis was performed solely on the basis of a holo-CRABP structure comparison (Fig. S8). Three residues—amino acids 75, 81, and 102—were selected for mutagenesis. Notably, these mutations to CRABPs have been made previously to identify the region of CRABP-2 that mediates the interaction with the RAR (19). As in the case of P450 27C1, holo-CRABP-2 can transfer atRA to RAR but holo-CRABP-1 cannot. In the case of RAR, it was found that these three residues were necessary and sufficient to mediate the interaction of CRABPs with RAR. CRABP-1, with the corresponding residues from CRABP-2 (Glu-75, Lys-81, Glu-102), was able to transfer atRA to RAR; CRABP-2 with the corresponding residues from CRABP-1 (Gln-75, Pro-81, Lys-102) was no longer able to. With P450 27C1, this did not occur. Steady-state kinetic analyses with these two mutant proteins resembled that of the WT proteins (Fig. S9). These results suggest that different (or additional) residues are required to mediate the interactions of CRABPs with P450 27C1 in comparison with RAR. The molecular basis for the functional difference between CRABP-1 and CRABP-2 in delivery of atRA to P450 27C1 remains unknown.

Regulation of P450 27C1 activity by apo-CRBPs was also assessed (Fig. 8). The effects of apo-CRBPs on P450 27C1 retinoid desaturation was substrate dependent, with the amount of inhibition varying from 0 to 100%. Previously, the plateau in inhibition after the ratio of binding protein:retinoid exceeded 1, as observed with P450 27C1 and atROL desaturation with excess apo-CRBP-1, was proposed to indicate allosteric modulation or inhibition of P450-mediated retinoid metabolism (6). For apo-CRABPs, the K_i values were less than the K_m for the reactions of P450 27C1 with the holo-CRABPs. This has previously been suggested to be due to differential recognition of apo-binding and holo-binding proteins by metabolic enzymes (3). If this was the case with P450 27C1, apo-cellular retinoid-binding proteins may inhibit desaturation even if they do not bind the retinoids present in the reaction (*i.e.*, apo-CRABPs should inhibit atROL and retinaldehyde desaturation, and apo-CRBP should inhibit atRA desaturation). To examine this possibility, additional assays were done with excess apo-CRBPs that did not bind the retinoid in the reaction (Fig. 9, *A*–*C*). No inhibition was observed in any of these conditions, suggesting that apo-CRBPs do not cause P450 27C1 inhibition through allosteric modulation. The possibility of apo-CRBPs competing with holo-CRBPs for binding to P450 27C1 was also considered. To address this, holo-CRBP-1 or holo-CRABP-2 was used to initiate reactions containing excess apo-CRBPs. Again, no inhibition was observed with each apo-CRBPs unless it could bind the retinoid in the reaction. Of note, the activity observed with increasing concentrations of apo-CRBP-1 supports our conclusion about the interaction of holo-CRBP-1 with P450 27C1, as the amount of product formed in these assays surpasses what would be predicted by the free ligand model (Fig. S10, *A* and *B*). With atRAL, where the steady-state kinetics of product formation do not appear largely different from the free ligand prediction (Fig. S4) due to the low K_m of retinoid desaturation and relatively high K_d of binding to

CRBP-1 (Table S3), apo-CRBP-1 inhibition results provide additional support for substrate channeling.

Some results from this study were surprising and are still not fully understood. While not unprecedented (*i.e.*, RAR specificity (19)), given the similarity of CRABP-1 and CRABP-2 and the ability of both proteins to interact with the CYP26 enzymes (5, 6), the difference in the ability of P450 27C1 to interact with CRABP-1 and CRABP-2 was unexpected. Despite our efforts, the basis of the difference in specificity remains unknown. In addition, the mechanism by which apo-cellular retinoid-binding proteins inhibit P450 27C1 desaturation is unclear. Previous work has suggested that the retinoid-binding ability of the protein was not required, and that inhibition may occur through allosteric modulation or competition with holo-binding proteins. Our results suggest that these two mechanisms do not generally occur with P450 27C1, but our results are consistent with the hypothesis that inhibition does not occur purely through retinoid sequestration (as would be predicted by the free ligand model, Fig. S10). Also of note, there is a lack of inhibition with atRAL (Figs. 8 and 9). One possibility is that the interaction interface between P450 27C1 and each holo-CRBP is different and that only the corresponding apo-CRBP can bind to the same site as the holo-CRBP. Alternatively, apo-CRBPs could specifically interact with the corresponding holo-CRBP and prevent transfer to P450 27C1. Without additional evidence, we cannot prove an alternate mechanism of apo-CRBP inhibition.

To our knowledge, this is the first study characterizing the interactions of a mitochondrial retinoid metabolizing enzyme with cellular retinoid-binding proteins. The mitochondrial localization of P450 27C1 is based on its requirement of Adx and NADPH–Adx reductase (AdR) for catalysis (10) and the presence of a putative mitochondrial translocation sequence (9). Previous work of this nature has focused on interactions with proteins that are generally expressed in the endoplasmic reticulum (ER) (CYP26 enzymes (5, 6), retinol dehydrogenases (26), retinaldehyde dehydrogenases (27), LRAT (3)), cytosol (retinaldehyde dehydrogenase (28)), or nucleus (RAR (15)). Cellular retinoid-binding proteins are soluble proteins and largely considered cytoplasmic, but it is well known that they can localize to other areas within the cell (*i.e.*, nucleus, ER-associated). Some studies have suggested that retinoid-binding proteins may also localize to the mitochondria. CRBP-1 has been shown to colocalize with mitochondrial markers in cell immunofluorescence studies (29), and CRBP and CRABP have previously been shown to cosediment with mitochondria (30, 31). The localization of retinoid-binding proteins within the mitochondria is currently unknown, but potential presence within the intermembrane space has been proposed (31). Mitochondrial P450s are cytoplasmically synthesized and then are generally thought to be inserted into the inner membrane of the mitochondria after cleavage, with the protein residing in the intermembrane space (32), thus potentially colocalizing with CRBPs. The mechanism of cellular retinoid-binding protein localization to the mitochondria has not been characterized. Some studies have shown that cellular retinoid-binding proteins can become post-translationally modified when localizing to different subcellular areas (*e.g.*, nuclear localization of CRABP-2 after SUMOylation (33)). No modifications have been identified with mitochondria-localized cellular retinoid-binding proteins, but if they are present, these may affect the interaction with P450 27C1 *in vivo*.

The majority of retinoid-metabolizing enzymes are localized to the ER. Outside of P450 27C1, the only mitochondrial retinoid-metabolizing enzyme that has been identified to our knowledge is retinol dehydrogenase 13 (RDH13), which catalyzes the reduction of atRAL (34). Like mitochondrial P450s, RDH13 is associated with the inner mitochondrial membrane, facing the intermembrane space. The ability of RDH13 to interact with retinoid-binding proteins has not been assessed. Some isoforms of RAR have even been found in mitochondria (35), and direct RAR regulation of mitochondrial transcription has been proposed (36). Although mitochondria have historically not been considered to have roles in retinoid function or metabolism, the presence of retinoid-binding proteins, RARs, and metabolic enzymes suggests a potential unknown biological importance of retinoids in mitochondrial function or the mitochondria in retinoid metabolism.

The ability of P450s to interact with cellular retinoid-binding proteins to receive substrates raises interesting questions about the potential for other P450–shuttle protein interactions. CRBPs and CRABPs are members of the intracellular lipid-binding protein family of proteins. Within this family is also the fatty acid–binding proteins (FABPs). Like retinoid-binding proteins, FABPs can directly interact with nuclear receptors (peroxisome proliferator-activated receptors) (37–39) and some metabolic enzymes (hormone-sensitive lipase) (40). Many P450s oxidize fatty acids (8), but to our knowledge, potential interactions between P450s and FABPs have not been investigated. These shuttle proteins may have the potential to directly interact with P450s and regulate metabolism *in vivo*. Alternatively, they may sequester ligands from P450s that have been identified as metabolic enzymes *in vitro*, limiting the contributions of these P450s to *in vivo* metabolism.

In summary, both holo-CRBP-1 and holo-CRABP-2 appear to directly channel retinoid ligands to P450 27C1. The rate of the P450 27C1 desaturation reaction when utilizing these holo-CRBPs as substrates is limited by the rate of retinoid transfer from the binding protein to the P450. In addition, P450 27C1 activity can be regulated by the level of apo-CRBP present; increased concentrations of apo-CRBPs typically inhibit P450 27C1 desaturation. The ability of P450 27C1 to interact with cellular retinoid-binding proteins supports its identification as an *in vivo* retinoid desaturase.

Experimental procedures

Reagents

Retinoids

atROL, all-*trans* retinal (atRAL), and atRA were purchased from Sigma-Aldrich or Toronto Research Laboratories.

3,4-Dehydroretinaldehyde, 3,4-dehydroretinol, all-*trans* retinol-d_5, all-*trans* retinal-d_5, and all-*trans* retinoic acid-d_5 were purchased from Toronto Research Laboratories. ddRA was purchased from Santa Cruz Biotechnology. All retinoid stocks were prepared fresh in absolute ethanol and kept in amber glass. Stock concentrations were determined spectrophotometrically based on extinction coefficients for each retinoid in ethanol (extinction coefficients listed in Table S1, see representative spectra in Fig. S2) (41). Hamilton glass syringes were used to prepare retinoid solutions. Solid stocks were stored under argon at −80 °C once opened.

Other reagents

Nickel–nitriloacetic acid (Ni-NTA) agarose was from QIAGEN. NuPAGE 10% Bis-Tris Gels, SimplyBlue SafeStain, NuPAGE MES and MOPS SDS Running Buffer, and 4 × NuPAGE LDS Sample Buffer were from Invitrogen (now Thermo Fisher Scientific). EDC and *N*-hydroxysulfosuccinimide were from Thermo Scientific and glycerol was from Fisher Scientific (both part of Thermo Fisher Scientific). Dialysis tubing was from Spectrum Spectra/Por. Thrombin, Sephadex G-75 resin, and 5 ml HiTrap Desalting columns were from GE Healthcare Life Sciences (now Cytiva). Amicon Ultra Centrifugal Filters, NADPH, 1,2-dilauroyl-*sn*-glycero-3-phosphocholine, IPTG, HPLC grade solvents, and all other reagents were purchased from Millipore Sigma/Sigma-Aldrich.

Recombinant proteins

P450 27C1 expression and purification

P450 27C1 was expressed and purified as previously described, with the following specifications: construct #3, N terminus modified, residues 3 to 60 deleted with expression-optimized sequence (42). DH5α Max Efficiency *Escherichia coli* competent cells (Invitrogen) were transformed with the P450 27C1 and pGro (GroEL/ES) plasmids and grown on Difco LB agar plates containing ampicillin (100 μg/ml) and kanamycin (50 μg/ml). An individual colony was used to inoculate LB broth (100 ml) containing ampicillin (100 μg/ml) and kanamycin (50 μg/ml) in a 250-ml Erlenmeyer flask. The solution was incubated overnight at 37 °C and 220 rpm. Overnight culture (5 ml) was used to inoculate TB media bulk culture (500 ml) containing ampicillin (100 μg/ml), kanamycin (50 μg/ml), trace elements (0.025% v/v), and glycerol (0.4% v/v) in a 2.8-l Fernbach flask. Bulk LB cultures were incubated at 37 °C and 250 rpm until they reached an OD_{600} of 0.6. At this point, expression of P450 27C1 was induced by addition of IPTG (1 mM, final). Expression of GroEL/ES was induced by the addition of solid L-(+)-arabinose (4 g/l). 5-Aminolevulinic acid hydrochloride (1 mM, final) was also added at the time of induction to promote heme synthesis. Flasks were incubated at 27 °C and 190 rpm for 40 h. Cells were pelleted by centrifugation at 5000*g*, 4 °C, for 20 min and stored at −80 °C.

Cell pellets were thawed on ice, resuspended in 2 × TES (15 ml/g pellet; 150 mM Tris HCl buffer (pH 7.4) containing 0.5 M sucrose and 0.1 mM EDTA), lysozyme (60 μl of 50 mg/ml solution/g pellet), and water (15 ml/g pellet) and stirred at 4 °C for 30 min. This solution was centrifuged at 5000*g* (4 °C) for 20 min, and the supernatant was discarded to isolate spheroplasts. Spheroplasts were resuspended in the sonication buffer (300 mM potassium phosphate (pH 7.4), 20% glycerol (v/v), 6 mM magnesium acetate) with protease inhibitor tablets and PMSF (1 mM, final) and sonicated with a 3/8-inch tip on a Branson Digital Sonifier Model 450 (VWR) at 80% power in 30-s bursts on ice for 5 to 6 cycles. The solution was centrifuged at 10,000*g* (4 °C) for 20 min, and the supernatant was centrifuged again at 100,000*g* (4 °C) for 1.5 h. The pellets were resuspended in 100 ml of solubilization buffer (300 mM potassium phosphate (pH 7.4), 20% glycerol (v/v), 1.5% CHAPS (w/v)) by stirring overnight at 4 °C. This solubilized solution was centrifuged at 100,000*g*, 4 °C for 30 min. The supernatant was loaded onto a 2.5-cm diameter open-bed glass column containing 10-ml Ni-NTA agarose resin equilibrated with 300 mM potassium phosphate buffer (pH 7.4) containing 20% glycerol (v/v) and 10 mM imidazole using a peristaltic pump. The column was then washed with 20 column volumes of wash buffer 1 (300 mM potassium phosphate (pH 7.4) containing 20% glycerol (v/v), 0.5% CHAPS (w/v), and 20 mM imidazole) and five column volumes of wash buffer 2 (300 mM potassium phosphate (pH 7.4) containing 20% glycerol (v/v) and 50 mM imidazole). Proteins were eluted in 25 4-ml fractions using the elution buffer (300 mM potassium phosphate (pH 7.4) containing 20% glycerol (v/v) and 300 mM imidazole). Fractions were pooled, and EDTA was added (1 mM final) before dialysis against 100 mM potassium phosphate (pH 7.4) containing 20% glycerol (v/v) and 0.1 mM EDTA (three times, 100 × volume). The concentration of the final dialyzed protein was determined by method of Omura and Sato (43), and the yield was ∼85 nmol/l bulk culture. Final protein purity was assessed by SDS-PAGE (Fig. S1).

Redox partner expression and purification

Bovine Adx and AdR were expressed in *E. coli* and purified as described previously (44, 45). Final protein purity was assessed by SDS-PAGE (Fig. S1).

Retinoid-binding protein expression

The plasmid for human CRBP-1 (pD441 plasmid with a 6-His C-terminal tag) was obtained from Dr Marcin Golczak (Case Western Reserve University). The vectors for CRABP-1 and CRABP-2 (pET28a vectors with 6-His N-terminal tag, removable by thrombin cleavage) were obtained from Dr Nina Isoherranen (University of Washington). Vectors for the CRABP mutants, CRABP-1 E75Q/K81P/E102K and CRABP-2 Q75E/P81K/K102E, were prepared by site-directed mutagenesis by GenScript. Final protein construct sequences are listed in Table S2. Expression and purification are based on the methods in Zhong *et al.* and Silvaroli *et al.*, with the following modifications (6, 46). Mutant CRABP proteins were prepared the same as described for WT proteins. Retinoid-binding proteins were transformed into *E. coli* strain BL21 (DE3)

Gold (Agilent) and grown on Difco LB agar plates containing kanamycin (20 μg/ml). An individual colony was used to inoculate 100 ml of LB broth containing kanamycin (50 μg/ml) in a 250-ml Erlenmeyer flask. The solution was incubated overnight at 37 °C with shaking at 220 rpm. Overnight culture (5 ml) was used to inoculate LB media bulk culture (500 ml) containing kanamycin (50 μg/ml) in a 2.8-l Fernbach flask. Bulk LB cultures were incubated at 37 °C and 250 rpm. When the bulk culture reached an OD_{600} of 0.6, expression of retinoid-binding proteins was induced with either 0.5 mM (CRBP-1) or 1 mM (CRABP-1, CRABP-2) IPTG. After 2 (CRABP-1, CRABP-2) or 4 (CRBP-1) h, cells were pelleted by centrifugation at 5000*g* for 15 min at 4 °C. Pellets were stored at −80 °C until workup.

CRBP-1 purification

Cells from bulk cultures (3 l) were thawed on ice and resuspended in 120 ml of the lysis buffer (20 mM Tris HCl buffer (pH 7.4) containing 500 mM NaCl and 5 mM imidazole) with lysozyme (1 mg/ml). Resuspended pellets were incubated with stirring for 30 min at 4 °C and then sonicated on ice using a 3/8-inch tip on a Branson Digital Sonifier Model 450 (VWR), set at 80% power for three cycles of 30 s with 1-min intermissions. The solution was then centrifuged at 15,000*g* for 30 min at 4 °C. The supernatant was applied to a 2.5-cm diameter open-bed glass column containing 10 ml of Ni-NTA agarose resin equilibrated in the lysis buffer by peristaltic pump with a flow rate of 2 ml/min. The resin was then washed with five column volumes of lysis buffer and five column volumes of wash buffer (20 mM Tris HCl buffer (pH 7.4) containing 500 mM NaCl and 30 mM imidazole), and then, proteins were eluted into 40 1-ml fractions with four column volumes of elution buffer (20 mM Tris HCl buffer (pH 7.4) containing 500 mM NaCl and 250 mM imidazole). Aliquots of each fraction were analyzed on a NuPAGE 10% Bis-Tris SDS-PAGE gel with MES running buffer to identify fractions that contained CRBP-1 (16 kDa band) (Fig. S1). Fractions containing purified CRBP-1 were pooled, concentrated, and buffer-exchanged into storage buffer (20 mM Tris HCl (pH 8.0) containing 10% glycerol (v/v)) using an Amicon Ultra 3K centrifugal filter device. The final CRBP-1 concentration was calculated using the molar extinction coefficient of ε_{280} = 26,470 M^{-1} cm^{-1}. The yield was ∼500 nmol/l of bulk culture. Proteins were aliquoted and stored at −80 °C.

CRABP-1 and CRABP-2 purification

The harvest and Ni-NTA purification of the CRABPs were similar to CRBP-1, with the following exceptions: 50 ml of the lysis buffer (for 3 l bulk culture) was used, and PMSF (1 mM) and EDTA-free protease inhibitor tablets (two mini-tablets, Roche) were added; sonication was done at 75% power for five rounds of 10 s with 30-s intermissions, and centrifugation was done at 20,000*g*. Fractions containing CRABPs were pooled and dialyzed four times (3000 MWCO tubing) against 50 volumes of 20 mM Tris HCl buffer (pH 7.4) containing 500 mM NaCl to remove imidazole. CRABP-1 and CRABP-2 (∼17 kDa) were located using SDS-PAGE. Mutant CRABP proteins were prepared as described for WT proteins. The concentrations of CRABPs were calculated based on molar extinction coefficients of ε_{280} = 20,970 M^{-1} cm^{-1} and ε_{280} = 19,480 M^{-1} cm^{-1} for CRABP-1 and CRABP-2, respectively. The yields were ∼2000 nmol/l bulk culture for both WT proteins. The yields for the mutant proteins were 500 nmol/l (CRABP-1 Q75E/P81K/K102E) and 1400 nmol/l (CRABP-2 E75Q/K81P/E102K). Proteins were stored at −80 °C with 10% glycerol (v/v) before thrombin digestion.

Stored CRABPs were thawed on ice and incubated with bovine thrombin overnight at 4 °C (0.03 U per 10 μg of CRABP). Thrombin digestion was monitored and verified by SDS-PAGE. Approximately 500 ml of Sephadex G-75 was prepared in a 2.5 cm × 100 cm open-bed glass column. A peristaltic pump was used to maintain a flow rate of ∼0.4 to 0.6 ml/min. The column was washed with one column volume of HEDK buffer (10 mM Hepes (pH 8.0) containing 100 mM KCl, 0.1 mM EDTA, and 0.5 mM DTT). The thrombin-digested CRABPs were loaded onto the column and eluted in ∼15-ml fractions over one column volume with the HEDK buffer. Aliquots of each fraction were placed into a 96-well UV-Star microplate (Greiner Bio-One) and analyzed for A_{280} using a BioTek plate reader (now part of Agilent Technologies). Fractions containing protein by this measurement were analyzed using a NuPAGE 10% Bis-Tris SDS-PAGE gel with MES running buffer to identify fractions that contained the thrombin-cleaved CRABP products (∼16 kDa and 15 kDa, for CRABP-1 and 2, respectively, Fig. S1). Fractions containing CRABPs were pooled and concentrated using an Amicon Ultra 3K centrifugal device. The final CRABP-1 concentration was calculated using the molar extinction coefficient of ε_{280} = 20,970 M^{-1} cm^{-1}. The yield was ∼500 nmol/l bulk culture (∼25% recovery). The final CRABP-2 concentration was calculated using the molar extinction coefficient of ε_{280} = 19,480 M^{-1} cm^{-1}. The yield was ∼2200 nmol/l bulk culture (∼100% recovery). The yield for the mutant proteins was 370 nmol/l (∼77% yield, CRABP-1 Q75E/P81K/K102E) and 1000 nmol/l (∼70% yield, CRABP-2 E75Q/K81P/E102K). Proteins were aliquoted and stored at −80 °C with 10% glycerol (v/v) added.

Preparation of holo-CRBPs

Holo-CRBPs were prepared immediately before assays by incubating apo-CRBPs with a 2.5-fold molar excess of retinoid for 30 min on ice (<2% ethanol final, v/v) in 50 mM potassium phosphate (pH 7.4) buffer containing 25 mM NaCl. The CRBP-retinoid solution was then centrifuged at 25,000*g* for 20 min at 4 °C. The supernatant was applied to a 5 ml HiTrap Desalting column with a syringe, according to manufacturer's instructions. Absorbance spectra of purified holo-CRBPs were recorded from 220 to 500 nm to ensure retinoid binding (representative spectra in Fig. S2). The concentration of each

holo-CRBP was calculated using previously determined extinction coefficients (see Table S1).

Catalytic assays

Steady-state kinetics of P450 27C1 retinoid metabolism with CRBPs

Incubations for P450 27C1 desaturation reactions were done similarly as previously described, with the following specifications (9, 10). Reactions were done in amber vials and contained 0.02 μM human P450 27C1, 5 μM bovine Adx, 0.2 μM bovine AdR, 16 μM 1,2-dilauroyl-*sn*-glycero-3-phosphocholine, and 1 mM NADPH in 50 mM potassium phosphate buffer (pH 7.4). Samples were preincubated at 37 °C for 5 min in a shaking water bath before the addition of retinoid (100% ethanol stock) or holo-CRBP to initiate the reaction (0–4 μM, final). The final reaction volume was 500 μl (≤1% ethanol, final, v/v). One minute after initiation, reactions were quenched by vortex mixing with 1 ml *tert*-butyl methyl ether containing 20 μM butylated hydroxytoluene and were then placed on ice. An aliquot (0.7 ml) of the top layer was removed and transferred to a 1.5-ml amber vial. Samples were dried under N_2 and resuspended in 50 μl ethanol and 50 μl of water (50% (v/v) ethanol, final) for analysis. Experiments were performed in duplicate.

Aliquots of each sample (20 μl) were analyzed by UPLC with a Waters Acquity system on an Acquity BEH octadecylsilane (C_{18}) column (1.7 μm; 2.1 mm × 100 mm) at 40 °C with a flow rate of 0.5 ml/min. Solvent A was 95% water, 4.9% CH_3CN, and 0.1% HCO_2H, and solvent B was 95% CH_3CN, 4.9% water, and 0.1% HCO_2H (all v/v/v). The solvent gradient used was as follows: 0 to 0.1 min, 40% A; 5 to 6 min, 25% A; 6.5 to 8 min, 0% A; 8.5 to 10 min, 40% A. Retinoids were identified by coelution with commercial standards, and quantification was based on A_{350} (3,4-dehydroretinol), A_{401} (3,4-dehydroretinaldehyde), and A_{370} (ddRA) peak areas. Example chromatograms are shown in Fig. S3. Peak areas were transformed to moles using an external standard curve prepared for each dehydroretinoid product. Data were analyzed with hyperbolic fits solving for k_{cat} and k_{cat}/K_m (k_{sp}) directly (47) (Equations 1 and 2) in Prism software (GraphPad).

$$v_0 = \frac{k_{sp}[S]}{1+\frac{k_{sp}[S]}{k_{cat}}} \quad (1)$$

$$k_{sp} = \frac{k_{cat}}{K_m} \quad (2)$$

Results from holo-CRBP assays were compared with the calculated kinetics of product formation under the assumption that P450 27C1 is only able to metabolize free retinoid in solution. The amount of free retinoid ($[R]_f$) in solution was calculated using the quadratic binding equation (Equation 3), as reported (5), where $[CRBP]_T$ is the total amount of binding protein, $[R]_T$ is the total amount of retinoid in the reaction, and the K_d is the binding affinity for the retinoid to the binding protein. The K_d values used for calculations were those previously reported (Table S3). Calculated free retinoid concentrations were input into Equation 1 to determine product formation.

$$[R]_f = \frac{\sqrt{([CRBP]_T-[R]_T+K_d)^2+4K_d[R]_T}-([CRBP]_T-[R]_T+K_d)}{2} \quad (3)$$

Isotope dilution channeling experiments

Reactions were performed as described above with the following specifications: reactions were initiated by the simultaneous addition of free atRA (d_5, 10 μM) and holo-CRABP-1 or holo-CRABP-2 (d_0, 10 μM), and reaction times ranged from 30 s to 180 s. An additional 1 μM concentration of the respective apo-CRABP was added to the holo-CRABP preparation to ensure that no free d_0-all-*trans* retinoic acid was added to the reaction. Reactions were performed with free d_0-and d_5-all-*trans* retinoic acid to determine how much the reaction rate was altered by the presence of the isotope labels (4,4,18,18,18-d_5-all-*trans* retinoic acid, positions labeled in Fig. 2). A small change in the catalytic rate has previously been observed with the P450 27C1 desaturation of 4,4-d_2-all-*trans* retinol (9). The other deuterium labels are not likely to lead to catalytic rate changes, given that P450 27C1 does not oxidize the 18th position. Experiments were performed in duplicate.

LC-MS/MS analysis was performed with the same chromatography system described above for other catalytic assays. A Thermo LTQ XL-Orbitrap mass spectrometer was operated with atmosphere pressure chemical ionization in a positive-ion mode and 15,000 resolution. The mass spectrometer was tuned with atRA. The tune settings were as follows: sheath gas flow rate, 40; auxiliary gas flow rate, 20; capillary temperature, 275 °C; atmosphere pressure chemical ionization vaporizer temperature, 400 °C; discharge current, 15 μA; capillary voltage, 2.5 V; tube lens, 45 V. For the multiple reaction monitoring mode, the isolation width was 2 *m/z* and the collision energy was 35. Transitions used for quantification are shown in Table S4, and example mass spectra and extracted ion chromatograms are shown in Fig. S5. Relative product formation was calculated by dividing the product peak area with the sum of the substrate and product peak areas. Product formation from the d_5-all-*trans* retinoic acid was corrected by dividing the value by the fraction of d_5/d_0 product formation in control incubations with free retinoids.

Effects of excess apo-CRBP

Reactions were performed as described above with the following differences: 0 to 2.5 μM apo-CRBP (up to 5 × the concentration of retinoid) was added, and the reaction was initiated with a 0.5 μM concentration of free retinoid or holo-CRBP. Experiments were performed in duplicate. Sample analysis was performed as described above. Relative product

formation was calculated by dividing the product peak area by the sum of the substrate and product peak areas. Percent activity was calculated relative to a reaction that did not contain apo-CRBP.

K_i values were calculated in GraphPad Prism using the Morrison quadratic equation (Equation 4). In this equation, y is the activity, v_0 is the activity in the absence of inhibitor, E_t is the concentration of enzyme, x is the concentration of inhibitor, S is the concentration of substrate, K_i is the inhibition constant, and K_m is the Michaelis–Menten constant determined in an experiment without the competitor (excess apo-CRBP). Values for E_t, S, and K_m were all fixed during fitting.

$$y = v_0 * \frac{1-\sqrt{\left([E_t]+x+K_i\left(1+\frac{[S]}{K_m}\right)\right)-\left([E_t]+x+K_i\left(1+\frac{[S]}{K_m}\right)\right)^2-4[E_t]*x}}{2[E_t]} \quad (4)$$

Binding studies

Substrate binding/transfer

To estimate apparent k_{on} values, P450 27C1 (1 μM, final) was mixed with each retinoid substrate (1 μM, final, free retinoid or holo-CRBP) in 200 mM potassium phosphate buffer (pH 7.4). Assays with free retinoid included Adx (15 μM, final). Measurements were made at 23 °C using an Olis RSM-1000 stopped-flow spectrophotometer (On-Line Instrument Systems). The settings and instrument configurations were as follows: wavelength range: 330 to 535 nm; slit widths: 1.24 mm; pathlength: 20 mm; gratings: 400 lines/mm, 500 nm blaze. For free substrates, spectra were recorded for 4 s after mixing (1000 spectra/s). For holo-CRBPs, spectra were recorded over a longer period (1000 s with 2 spectra/s). Absorbance readings at 390 and 420 nm were extracted from the spectra, and then, ΔA_{390}-A_{420} was calculated at each time point. Traces were averaged using the Olis GlobalWorks software. Absorbance differences were corrected to make the initial A_{390}-A_{420} value 0. Mixing transients were fit by nonlinear regression in GraphPad Prism as reported previously with Equation 5 (48). Pretrigger data are shown (pre–zero time data) but are not used for fitting. In this equation, y is the observed absorbance difference, A is a scaling constant, C_0 is the initial concentration of the enzyme/substrate, k is the binding rate constant, and x is time.

$$y = A * \left(\frac{-[C_0]}{[C_0]*k*x+1}+[C_0]\right) \quad (5)$$

To determine if the rate of retinoid transfer from holo-CRBPs was dependent on the P450 27C1 concentration, holo-CRABPs (1 μM, with 0.1 μM excess apo-protein) were mixed with varying amounts of P450 27C1 (1–5 μM) in the presence of Adx (15 μM) in 200 mM potassium phosphate buffer (pH 7.4). Measurements were made at 23 °C using an Olis computerized HP 8452 Diode Array. Spectra were recorded from 350 to 500 nm for 1000 s with 1-s integration time. Absorbance readings at 390 and 420 nm were extracted from the spectra, and ΔA_{390}-A_{420} was calculated at each time point using the Olis GlobalWorks software. Absorbance differences were corrected to make the initial value zero. Binding constants were calculated in GraphPad Prism using a modified single-exponential one-phase association equation (Equation 6) or a biexponential two-phase association equation (Equation 7). In these equations, y is the measured absorbance difference, y_{max} is the plateau value, $span_{fast}$ and $span_{slow}$ are the percentages accounted for by each exponential component multiplied by y_{max}, k is the binding rate constant, and x is time.

$$y = y_{max}\left(1-e^{-kx}\right) \quad (6)$$

$$y = span_{fast}\left(1-e^{-k_{fast}x}\right)+span_{slow}\left(1-e^{-k_{slow}x}\right) \quad (7)$$

Protein–protein interaction studies

CRABPs (20 μM final, apo-proteins and holo-proteins) were incubated at 23 °C with shaking with EDC (2 mM) and *N*-hydroxysulfosuccinimide (5 mM) in 100 mM potassium phosphate buffer (pH 7.4) for 15 min. P450 (2 μM, final) was added and then the samples were incubated at 23 °C with shaking for an additional 2 h. The final reaction volume was 20 μl. To quench the reactions, an equal volume of 2 × Laemmli buffer (with β-mercaptoethanol) was added, and the samples were heated at 90 °C for 10 min. Controls were performed with P450 27C1 and Adx (positive control) and with P450 3A4 (expressed and purified as described previously (49, 50)) and holo-CRABPs (negative control). In addition, cross-linking incubations were performed with individual proteins, and an additional incubation was performed without the cross-linking reagent to allow for identification of bands that are due to heteroprotein complexes. Samples were run on a NuPAGE 4 to 12% Bis-Tris SDS-PAGE gel with Mops running buffer and stained with SimplyBlue SafeStain.

To identify structural differences that might lead to differences in interaction with P450 27C1, CRABP-1 and CRAPB-2 sequences were aligned in UniProt with Clustal Omega (51). The surface electrostatic potential of holo-CRABP-1 and holo-CRABP-2 was calculated using the APBS plugin (52) in PyMOL (53) using existing x-ray crystallography structures (PDB ID: 1CBR, 1CBS) (54).

Data availability

All data are contained within the article and the Supporting Information.

Supporting information—This article contains supporting information (15, 41, 43, 51–68).

Acknowledgments—We thank T. T. N. Phan for preparation of P450 27C1, C. J. Wilkey and J. G. Chapman for preparation of AdR, M. Golczak for providing the plasmid for CRBP-1, N. Isoherranen and K. Yabut for providing the plasmids and the expression protocol for CRABP-1 and CRABP-2, the Vanderbilt University Mass Spectrometry Research Center for assistance with MS analysis, and K. Trisler for assistance in preparation of the manuscript.

Author contributions—S. M. G. conceptualization; S. M. G. investigation; S. M. G. formal analysis; S. M. G. and F. P. G. methodology; S. M. G. data curation; S. M. G. writing – original draft; F. P. G. supervision; F. P. G. writing – review and editing.

Funding and additional information—This work was supported by NIH Grants R01 GM118122 (to F. P. G.), T32 ES007028 (to F. P. G. for support of S. M. G.), and F31 AR077386 (to S. M. G.). This content is solely the responsibility of the authors and does not necessarily represent the official views of the National Institutes of Health.

Conflict of interest—The authors declare that they have no conflicts of interest with the contents of this article.

Abbreviations—The abbreviations used are: AdR, NADPH–adrenodoxin reductase; Adx, adrenodoxin; atRA, all-*trans* retinoic acid; atRAL, all-*trans* retinaldehyde; atROL, all-*trans* retinol; CRABP, cellular retinoic acid–binding protein; CRBP, cellular retinol-binding protein; CYP or P450, cytochrome P450; ddRA, 3,4-dehydroretinoic acid; EDC, 1-ethyl-3-(3-dimethylaminopropyl)carbodiimide hydrochloride; ER, endoplasmic reticulum; FABP, fatty acid–binding protein; LRAT, lecithin retinol acyltransferase; Ni-NTA, nickel–nitrilotriacetic acid; RAR, retinoic acid receptor; RDH13, retinol dehydrogenase 13.

References

1. Bernlohr, D. A., Simpson, M. A., Hertzel, A. V., and Banaszak, L. J. (1997) Intracellular lipid-binding proteins and their genes. *Annu. Rev. Nutr.* **17**, 277–303
2. Napoli, J. L. (2017) Cellular retinoid binding-proteins, CRBP, CRABP, FABP5: Effects on retinoid metabolism, function and related diseases. *Pharmacol. Ther.* **173**, 19–33
3. Herr, F. M., and Ong, D. E. (1992) Differential interaction of lecithin-retinol acyltransferase with cellular retinol binding proteins. *Biochemistry* **31**, 6748–6755
4. Boerman, M. H., and Napoli, J. L. (1991) Cholate-independent retinyl ester hydrolysis. Stimulation by apo-cellular retinol-binding protein. *J. Biol. Chem.* **266**, 22273–22278
5. Nelson, C. H., Peng, C. C., Lutz, J. D., Yeung, C. K., Zelter, A., and Isoherranen, N. (2016) Direct protein-protein interactions and substrate channeling between cellular retinoic acid binding proteins and CYP26B1. *FEBS Lett.* **590**, 2527–2535
6. Zhong, G., Ortiz, D., Zelter, A., Nath, A., and Isoherranen, N. (2018) CYP26C1 is a hydroxylase of multiple active retinoids and interacts with cellular retinoic acid binding proteins. *Mol. Pharmacol.* **93**, 489–503
7. Rendic, S., and Guengerich, F. P. (2015) Survey of human oxidoreductases and cytochrome P450 enzymes involved in the metabolism of xenobiotic and natural chemicals. *Chem. Res. Toxicol.* **28**, 38–42
8. Guengerich, F. P. (2015) Human cytochrome P450 enzymes. In: Ortiz de Montellano, P. R., ed. *Cytochrome P450: Structure, Mechanism, and Biochemistry*, 4th Ed, Springer, New York, NY: 523–785
9. Johnson, K. M., Phan, T. T. N., Albertolle, M. E., and Guengerich, F. P. (2017) Human mitochondrial cytochrome P450 27C1 is localized in skin and preferentially desaturates *trans*-retinol to 3,4-dehydroretinol. *J. Biol. Chem.* **292**, 13672–13687
10. Kramlinger, V. M., Nagy, L. D., Fujiwara, R., Johnson, K. M., Phan, T. T., Xiao, Y., Enright, J. M., Toomey, M. B., Corbo, J. C., and Guengerich, F. P. (2016) Human cytochrome P450 27C1 catalyzes 3,4-desaturation of retinoids. *FEBS Lett.* **590**, 1304–1312
11. Andersson, E., Björklind, C., Törmä, H., and Vahlquist, A. (1994) The metabolism of vitamin A to 3,4-didehydroretinol can be demonstrated in human keratinocytes, melanoma cells and HeLa cells, and is correlated to cellular retinoid-binding protein expression. *Biochim. Biophys. Acta* **1224**, 349–354
12. Vahlquist, A., Andersson, E., Coble, B. I., Rollman, O., and Törmä, H. (1996) Increased concentrations of 3,4-didehydroretinol and retinoic acid-binding protein (CRABPII) in human squamous cell carcinoma and keratoacanthoma but not in basal cell carcinoma of the skin. *J. Invest. Dermatol.* **106**, 1070–1074
13. Eller, M. S., Oleksiak, M. F., McQuaid, T. J., McAfee, S. G., and Gilchrest, B. A. (1992) The molecular cloning and expression of two CRABP cDNAs from human skin. *Exp. Cell Res.* **198**, 328–336
14. Siegenthaler, G., Saurat, J. H., Morin, C., and Hotz, R. (1984) Cellular retinol- and retinoic acid-binding proteins in the epidermis and dermis of normal human skin. *Br. J. Dermatol.* **111**, 647–654
15. Dong, D., Ruuska, S. E., Levinthal, D. J., and Noy, N. (1999) Distinct roles for cellular retinoic acid-binding proteins I and II in regulating signaling by retinoic acid. *J. Biol. Chem.* **274**, 23695–23698
16. Enright, J. M., Toomey, M. B., Sato, S.-Y., Temple, S. E., Allen, J. R., Fujiwara, R., Kramlinger, V. M., Nagy, L. D., Johnson, K. M., Xiao, Y., How, M. J., Johnson, S. L., Roberts, N. W., Kefalov, V. J., Guengerich, F. P., *et al.* (2015) Cyp27c1 red-shifts the spectral sensitivity of photoreceptors by converting vitamin A_1 into A_2. *Curr. Biol.* **25**, 3048–3057
17. Vahlquist, A., Lee, J. B., Michaëlsson, G., and Rollman, O. (1982) Vitamin A in human skin: II. Concentrations of carotene, retinol and dehydroretinol in various components of normal skin. *J. Invest. Dermatol.* **79**, 94–97
18. Aström, A., Tavakkol, A., Pettersson, U., Cromie, M., Elder, J. T., and Voorhees, J. J. (1991) Molecular cloning of two human cellular retinoic acid-binding proteins (CRABP). Retinoic acid-induced expression of CRABP-II but not CRABP-I in adult human skin *in vivo* and in skin fibroblasts *in vitro*. *J. Biol. Chem.* **266**, 17662–17666
19. Budhu, A., Gillilan, R., and Noy, N. (2001) Localization of the RAR interaction domain of cellular retinoic acid binding protein-II. *J. Mol. Biol.* **305**, 939–949
20. Budhu, A. S., and Noy, N. (2002) Direct channeling of retinoic acid between cellular retinoic acid-binding protein II and retinoic acid receptor sensitizes mammary carcinoma cells to retinoic acid-induced growth arrest. *Mol. Cell. Biol.* **22**, 2632–2641
21. Sjoelund, V., and Kaltashov, I. A. (2012) Modification of the zonal elution method for detection of transient protein–protein interactions involving ligand exchange. *Anal. Chem.* **84**, 4608–4612
22. Gao, Q., Doneanu, C. E., Shaffer, S. A., Adman, E. T., Goodlett, D. R., and Nelson, S. D. (2006) Identification of the interactions between cytochrome P450 2E1 and cytochrome b_5 by mass spectrometry and site-directed mutagenesis. *J. Biol. Chem.* **281**, 20404–20417
23. Kumar, A., and Estrada, D. F. (2019) Specificity of the redox complex between cytochrome P450 24A1 and adrenodoxin relies on carbon-25 hydroxylation of vitamin-D substrate. *Drug Metab. Dispos.* **47**, 974–982
24. Peng, H. M., and Auchus, R. J. (2017) Molecular recognition in mitochondrial cytochromes P450 that catalyze the terminal steps of corticosteroid biosynthesis. *Biochemistry* **56**, 2282–2293

25. Bumpus, N. N., and Hollenberg, P. F. (2010) Cross-linking of human cytochrome P450 2B6 to NADPH-cytochrome P450 reductase: Identification of a potential site of interaction. *J. Inorg. Biochem.* **104**, 485–488
26. Lapshina, E. A., Belyaeva, O. V., Chumakova, O. V., and Kedishvili, N. Y. (2003) Differential recognition of the free versus bound retinol by human microsomal retinol/sterol dehydrogenases: Characterization of the holo-CRBP dehydrogenase activity of RoDH-4. *Biochemistry* **42**, 776–784
27. Penzes, P., Wang, X., and Napoli, J. L. (1997) Enzymatic characteristics of retinal dehydrogenase type I expressed in *Escherichia coli*. *Biochim. Biophys. Acta* **1342**, 175–181
28. Posch, K. C., Burns, R. D., and Napoli, J. L. (1992) Biosynthesis of all-trans-retinoic acid from retinal. Recognition of retinal bound to cellular retinol binding protein (type I) as substrate by a purified cytosolic dehydrogenase. *J. Biol. Chem.* **267**, 19676–19682
29. Jiang, W., and Napoli, J. L. (2012) Reorganization of cellular retinol-binding protein type 1 and lecithin:retinol acyltransferase during retinyl ester biosynthesis. *Biochim. Biophys. Acta* **1820**, 859–869
30. Adachi, N., Smith, J. E., Sklan, D., and Goodman, D. S. (1981) Radioimmunoassay studies of the tissue distribution and subcellular localization of cellular retinol-binding protein in rats. *J. Biol. Chem.* **256**, 9471–9476
31. Ruff, S. J., and Ong, D. E. (2000) Cellular retinoic acid binding protein is associated with mitochondria. *FEBS Lett.* **487**, 282–286
32. Omura, T. (2006) Mitochondrial P450s. *Chem. Biol. Interact.* **163**, 86–93
33. Majumdar, A., Petrescu, A. D., Xiong, Y., and Noy, N. (2011) Nuclear translocation of cellular retinoic acid-binding protein II is regulated by retinoic acid-controlled SUMOylation. *J. Biol. Chem.* **286**, 42749–42757
34. Belyaeva, O. V., Korkina, O. V., Stetsenko, A. V., and Kedishvili, N. Y. (2008) Human retinol dehydrogenase 13 (RDH13) is a mitochondrial short-chain dehydrogenase/reductase with a retinaldehyde reductase activity. *FEBS J.* **275**, 138–147
35. Everts, H. B., Claassen, D. O., Hermoyian, C. L., and Berdanier, C. D. (2002) Nutrient-gene interactions: Dietary vitamin A and mitochondrial gene expression. *IUBMB Life* **53**, 295–301
36. Everts, H. B., and Berdanier, C. D. (2002) Regulation of mitochondrial gene expression by retinoids. *IUBMB Life* **54**, 45–49
37. Hostetler, H. A., McIntosh, A. L., Atshaves, B. P., Storey, S. M., Payne, H. R., Kier, A. B., and Schroeder, F. (2009) L-FABP directly interacts with PPARα in cultured primary hepatocytes. *J. Lipid Res.* **50**, 1663–1675
38. Tan, N.-S., Shaw Natacha, S., Vinckenbosch, N., Liu, P., Yasmin, R., Desvergne, B., Wahli, W., and Noy, N. (2002) Selective cooperation between fatty acid binding proteins and peroxisome proliferator-activated receptors in regulating transcription. *Mol. Cell. Biol.* **22**, 5114–5127
39. Velkov, T. (2013) Interactions between human liver fatty acid binding protein and peroxisome proliferator activated receptor selective drugs. *PPAR Res.* **2013**, 938401
40. Jenkins-Kruchten, A. E., Bennaars-Eiden, A., Ross, J. R., Shen, W.-J., Kraemer, F. B., and Bernlohr, D. A. (2003) Fatty acid-binding protein-hormone-sensitive lipase interaction: Fatty acid dependence on binding. *J. Biol. Chem.* **278**, 47636–47643
41. Barua, A. B., and Furr, H. C. (1998) Properties of retinoids. In: Redfern, C. P. F., ed. *Retinoid Protocols*, Humana Press, Totowa, NJ: 3–28
42. Wu, Z.-L., Bartleson, C. J., Ham, A.-J. L., and Guengerich, F. P. (2006) Heterologous expression, purification, and properties of human cytochrome P450 27C1. *Arch. Biochem. Biophys.* **445**, 138–146
43. Omura, T., and Sato, R. (1964) The carbon monoxide-binding pigment of liver microsomes. I. Evidence for its hemoprotein nature. *J. Biol. Chem.* **239**, 2370–2378
44. Palin, M. F., Berthiaume, L., Lehoux, J. G., Waterman, M. R., and Sygusch, J. (1992) Direct expression of mature bovine adrenodoxin in *Escherichia coli*. *Arch. Biochem. Biophys.* **295**, 126–131
45. Sagara, Y., Wada, A., Takata, Y., Waterman, M. R., Sekimizu, K., and Horiuchi, T. (1993) Direct expression of adrenodoxin reductase in *Escherichia coli* and the functional characterization. *Biol. Pharm. Bull.* **16**, 627–630
46. Silvaroli, J. A., Arne, J. M., Chelstowska, S., Kiser, P. D., Banerjee, S., and Golczak, M. (2016) Ligand binding induces conformational changes in human cellular retinol-binding protein 1 (CRBP1) revealed by atomic resolution crystal structures. *J. Biol. Chem.* **291**, 8528–8540
47. Johnson, K. A. (2019) New standards for collecting and fitting steady state kinetic data. *Beilstein J. Org. Chem.* **15**, 16–29
48. Reddish, M. J., and Guengerich, F. P. (2019) Human cytochrome P450 11B2 produces aldosterone by a processive mechanism due to the lactol form of the intermediate 18-hydroxycorticosterone. *J. Biol. Chem.* **294**, 12975–12991
49. Gillam, E. M., Baba, T., Kim, B. R., Ohmori, S., and Guengerich, F. P. (1993) Expression of modified human cytochrome P450 3A4 in *Escherichia coli* and purification and reconstitution of the enzyme. *Arch. Biochem. Biophys.* **305**, 123–131
50. Hosea, N. A., Miller, G. P., and Guengerich, F. P. (2000) Elucidation of distinct ligand binding sites for cytochrome P450 3A4. *Biochemistry* **39**, 5929–5939
51. Sievers, F., Wilm, A., Dineen, D., Gibson, T. J., Karplus, K., Li, W., Lopez, R., McWilliam, H., Remmert, M., Söding, J., Thompson, J. D., and Higgins, D. G. (2011) Fast, scalable generation of high-quality protein multiple sequence alignments using Clustal Omega. *Mol. Syst. Biol.* **7**, 539
52. Baker, N. A., Sept, D., Joseph, S., Holst, M. J., and McCammon, J. A. (2001) Electrostatics of nanosystems: Application to microtubules and the ribosome. *Proc. Natl. Acad. Sci. U. S. A.* **98**, 10037–10041
53. *The PyMOL Molecular Graphics System* (2nd Ed,. (2015) Schrodinger, LLC, New York, NY
54. Kleywegt, G. J., Bergfors, T., Senn, H., Le Motte, P., Gsell, B., Shudo, K., and Jones, T. A. (1994) Crystal structures of cellular retinoic acid binding proteins I and II in complex with all-*trans*-retinoic acid and a synthetic retinoid. *Structure* **2**, 1241–1258
55. Hubbard, R., Brown, P. K., and Bownds, D. (1971) Methodology of vitamin A and visual pigments. *Methods Enzymol.* **243**, 615–653
56. Robeson, C. D., Cawley, J. D., Weisler, L., Stern, M. H., Eddinger, C. C., and Chechak, A. J. (1955) Chemistry of vitamin A. XXIV. The synthesis of geometric isomers of vitamin A via methyl β-methylglutaconate1. *J. Am. Chem. Soc.* **77**, 4111–4119
57. Planta, C. V., Schweiter, U., Chopard-dit-Jean, L., Rüegg, R., Kofler, M., and Isler, O. (1962) Synthesen in der Vitamin-A2-Reihe. 4. Mitteilung. Physikalische Eigenschaften von isomeren Vitamin-A- und Vitamin-A2-Verbindungen. *Helv. Chim. Acta* **45**, 548–561
58. Akhrem, A. A., Lapko, V. N., Lapko, A. G., Shkumatov, V. M., and Chashchin, V. L. (1979) Isolation, structural organization and mechanism of action of mitochondrial steroid hydroxylating systems. *Acta Biol. Med. Ger.* **38**, 257–273
59. Kimura, T. (1968) Biochemical aspects of iron-sulfur linkage in non-heme iron protein, with special reference to "Adrenodoxin". In:*Structure and Bonding*, 5. Springer, Berlin, Heidelberg, 1–40
60. Gasteiger, E., Hoogland, C., Gattiker, A., Duvaud, S.e., Wilkins, M. R., Appel, R. D., and Bairoch, A. (2005) Protein identification and analysis tools on the ExPASy server. In: Walker, J. M., ed. *The Proteomics Protocols Handbook*, Humana Press, Totowa, NJ: 571–607
61. Ong, D. E. (1982) Purification and partial characterization of cellular retinol-binding protein from human liver. *Cancer Res.* **42**, 1033–1037
62. MacDonald, P. N., and Ong, D. E. (1987) Binding specificities of cellular retinol-binding protein and cellular retinol-binding protein, type II. *J. Biol. Chem.* **262**, 10550–10556
63. Ong, D. E., and Chytil, F. (1978) Cellular retinoic acid-binding protein from rat testis. Purification and characterization. *J. Biol. Chem.* **253**, 4551–4554
64. Fiorella, P. D., Giguère, V., and Napoli, J. L. (1993) Expression of cellular retinoic acid-binding protein (type II) in *Escherichia coli*. Characterization and comparison to cellular retinoic acid-binding protein (type I). *J. Biol. Chem.* **268**, 21545–21552
65. Folli, C., Calderone, V., Ottonello, S., Bolchi, A., Zanotti, G., Stoppini, M., and Berni, R. (2001) Identification, retinoid binding, and X-ray analysis of a human retinol-binding protein. *Proc. Natl. Acad. Sci. U. S. A.* **98**, 3710–3715

66. Kane, M. A., Bright, F. V., and Napoli, J. L. (2011) Binding affinities of CRBPI and CRBPII for 9-*cis*-retinoids. *Biochim. Biophys. Acta* **1810**, 514–518
67. Noy, N., and Blaner, W. S. (1991) Interactions of retinol with binding proteins: Studies with rat cellular retinol-binding protein and with rat retinol-binding protein. *Biochemistry* **30**, 6380–6386
68. Jones, J. W., Pierzchalski, K., Yu, J., and Kane, M. A. (2015) Use of fast HPLC multiple reaction monitoring cubed for endogenous retinoic acid quantification in complex matrices. *Anal. Chem.* **87**, 3222–3230
69. Roos, T. C., Jugert, F. K., Merk, H. F., and Bickers, D. R. (1998) Retinoid metabolism in the skin. *Pharmacol. Rev.* **50**, 315
70. Nomenclature of retinoids. *Pure Appl. Chem.* **55**, (1983), 721–726